

AD-775 745

A PHOTOELECTRIC PHOTOMETER FOR THE
Fe XIV SOLAR CORONA

Richard R. Fisher

Air Force Cambridge Research Laboratories
L. G. Hanscom Field, Massachusetts

9 November 1973

DISTRIBUTED BY:

NTIS

National Technical Information Service
U. S. DEPARTMENT OF COMMERCE
5285 Port Royal Road, Springfield Va. 22151

DISCLAIMER NOTICE

**THIS DOCUMENT IS BEST QUALITY
PRACTICABLE. THE COPY FURNISHED
TO DTIC CONTAINED A SIGNIFICANT
NUMBER OF PAGES WHICH DO NOT
REPRODUCE LEGIBLY.**

Unclassified

Security Classification

AD 775745

DOCUMENT CONTROL DATA - R&D		
(Security classification of title, body of abstract and indexing annotation must be entered when the overall report is classified)		
1. ORIGINATING ACTIVITY (Corporate author) Air Force Cambridge Research Laboratories (LM) L. G. Hanscom Field Bedford, Massachusetts 01730		2a. REPORT SECURITY CLASSIFICATION Unclassified
		2b. GROUP
3. REPORT TITLE A PHOTOELECTRIC PHOTOMETER FOR THE FE XIV SOLAR CORONA		
4. DESCRIPTIVE NOTES (Type of report and inclusive dates) Scientific. Interim		
5. AUTHOR(S) (First name, middle initial, last name) Richard R. Fisher		
8. REPORT DATE 9 November 1973	7a. TOTAL NO. OF PAGES 18/15	7b. NO. OF REFS 4
8a. CONTRACT OR GRANT NO.	9a. ORIGINATOR'S REPORT NUMBER(S) AFCRL-TR-73-0696	
b. PROJECT, TASK, WORK UNIT NOS. 76490701		
c. DOD ELEMENT 62101F	9b. OTHER REPORT NO(S) (Any other numbers that may be assigned this report)	
d. DOD SUBELEMENT 681000	IP, No. 205	
10. DISTRIBUTION STATEMENT Approved for public release; distribution unlimited		
11. SUPPLEMENTARY NOTES TECH, OTHER	12. SPONSORING MILITARY ACTIVITY Air Force Cambridge Research Laboratories (LM) L. G. Hanscom Field Bedford, Massachusetts 01730	
13. ABSTRACT A photoelectric photometer for the emission line 5303 (Fe XIV formed in regions where $T_e = 2.0 \times 10^6$ °K) of the solar corona is described in this paper. The emission line is isolated from the scattered light of the sky and the instrument by means of a rapid change in the bandpass of a birefringent filter. A piezoelectric variable retarder is used to accomplish the bandpass modification at a 100 kHz rate. The instrument is capable of detecting the corona in scattered light situations that exceed the maximum allowed for filter photography by a factor of 10; thus, the number of hours during which coronal observations can be made with the photoelectric instrument is significantly larger than the photographic method presently used. An example of synoptic observations of the Fe XIV corona is presented. Spatial resolution achieved is limited by the scan stop in the image plane and is 1.1 arc minutes. Scans are made in position angle, holding the scan distance from the limb a constant. The Fe XIV signal is detected out to a distance of $1.55 R/R_0$ above the limb. Reproduced by NATIONAL TECHNICAL INFORMATION SERVICE U S Department of Commerce Springfield VA 22151		

DD FORM 1473
1 NOV 65

Unclassified

Security Classification

Preface

The author wishes to express his appreciation to G. Spence, A. Marking, and A. Godard for their efforts in the construction and maintenance of the photometer. Dr. C. P. Catalano provided early assistance with the data reduction programs. This research was supported by AFCL, L. G. Hanscom Field, Bedford, Massachusetts.

Contents

1. INTRODUCTION	7
2. THE FILTER SYSTEM	8
3. DETECTION SYSTEM	11
4. RESULTS	12
5. CONCLUSIONS	15

Illustrations

1. A Schematic Diagram of the Optical Components of the Fe XIV Photometer	8
2. A Photoelectric Scan in Wavelength Showing the Photometer Transmission Profile With the Piezoelectric Modulator Operating	10
3. A Schematic Diagram of the Big Dome Spar Scan and Data Collection System as Used With the FE XIV Photometer System	11
4. An example of the Fe XIV Photometer Quick-Lock Reduction Program	13
5. A Series of Five Full Coronal Scans Separated in Time by About One Day Each	14

A Photoelectric Photometer for the Fe XIV Solar Corona

1. INTRODUCTION

The $\lambda 5303$ line of the solar corona, originating from Fe XIV, is the brightest line available to observers in the visible portion of the spectrum. By chopping between the neighboring continuum and this emission line, Lyot¹ was able to detect the corona photoelectrically for a case in which the coronal signal was small compared against the brightness of the scattered photospheric radiation. The same detection scheme, using a birefringent filter with a variable bandpass chopping between the spectral region of the emission line and the nearby continuum, was used by the author to detect the emission line corona out to a distance of 1.75 radii from the center of the solar disk. The improvement over Lyot's scheme is the addition of a rapid method of chopping and a phase-locked synchronous detection system. The major advantages of this photoelectric system are the increased temporal coverage of coronal data and an increased coverage in the spatial extent of the corona detected. Ordinary filter photography usually is not capable of showing the green line corona at heights above 1.30 R/R_0 . The major reduction in scattered light necessary to make a coronal

(Received for Publication 13 November 1973)

1. Lyot, B. (1950) C.R. Acad. Sci. Paris, 231:461.

observation is obtained by locating a coronagraph at a site where the sky is relatively free from aerosol. These requirements are clearly stated in an excellent review article by Evans.²

2. THE FILTER SYSTEM

The birefringent filter used in this photometer is OPL No. 34, a filter that can be used at $H\alpha$, the D_2 line of the He I, or $\lambda 5303$, the green line of Fe XIV. As usual, it is necessary to temperature control the filter; the temperature coefficient for the thickest calcite element is approximately $-0.3 \text{ \AA}/^\circ\text{C}$ at the green line. The full width at half maximum for the thickest element of the filter is 0.58 \AA . This narrow bandpass—narrow compared with the Doppler width of the green line of 0.7 \AA —is necessary in order to reduce the sensitivity of the equipment to Doppler displacements of the Fe absorption line in the scattered light spectrum. This problem is discussed below.

The arrangement of the filter system is shown in Figure 1. Light enters the photometer through a field stop in the image plane and passes through a

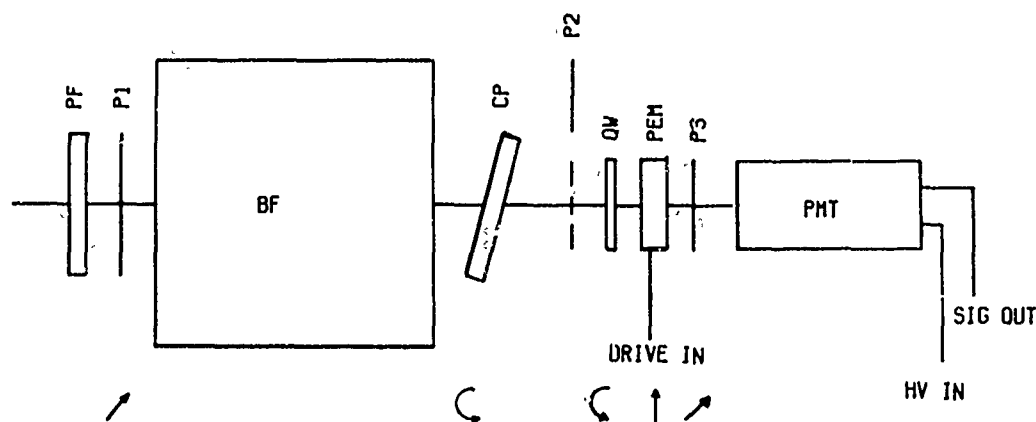


Figure 1. A Schematic Diagram of the Optical Components of the Fe XIV Photometer. PF: pre-filter (FWHM = 12 \AA). P1: Initial polaroid for the thickest element of the birefringent filter (BF). CP: parallel plate compensator. P2: calibration polaroid (removed for normal operation). QW: $\lambda/4$ plate (5600 \AA). P3: final polaroid of the birefringent filter. PEM: piezoelectric modulator

2. Evans, J. W. (1953) The Sun, University of Chicago Press, 635 pp.

multi-layer interference pre-filter into the birefringent filter. The front polaroid is so arranged that it may be rotated to provide limited tuning of the thickest element. The next-to-thickest element is physically placed last in the filter and the last polarizer removed. The beam then passes through a piezoelectric modulator³ adjusted so that the retardance varies from $+\lambda/2$ to $-\lambda/2$. A final polaroid is used to develop a single, time-variable bandpass. A parallel plate compensator is placed between the last element of the birefringent filter and the variable retarder. This compensator is used to achieve a null signal on an attenuated image of the center of the solar disk. For an ordinary birefringent filter the transmission is given by

$$T \propto \prod_{i=1}^N \cos^{i-1} \frac{\pi d_o (\epsilon - \omega)}{\lambda}, \quad (1)$$

where d_o is the thickness of the thinnest element, $\epsilon - \omega$ is the difference between the ordinary and extraordinary indices of refraction, and λ is the wavelength of interest. In the case of the above system, the transmission is time dependent, a function of the drive voltage on the modulator. If the voltage applied to the modulator is such that the retardance varies $\pm \lambda/2$ through zero, at a frequency of $2\pi w$, the transmission becomes

$$\begin{aligned} T & \propto \left(\prod_{i=1}^N \cos^2 \left(2^{i-1} \pi d_o \frac{(\epsilon - \omega)}{\lambda} \right) \right) \times \left(\cos^2 \left(2^{N+1} \pi d_o \frac{(\epsilon - \omega)}{\lambda} \right) \right) \\ & \times \left(\cos^2 \left[2^{N+2} \pi d_o \frac{(\epsilon - \omega)}{\lambda} \right] \right) \times \cos^2 (4\pi wt + \phi) \\ & + \sin^2 \left[2^{N+2} \pi d_o \frac{(\epsilon - \omega)}{\lambda} \right] \left(\sin^2 (4\pi wt + \phi) \right). \end{aligned} \quad (2)$$

The time averaged transmission of the filter is shown in Figure 2. The two side lobes are located well into the continuum of scattered light, while the central bandpass is located on the red wing of the 5303 line. There is an absorption line, multiplet 553 of Fe I, which is formed in the photosphere, located in the blue wing of the Fe XIV line. Long the base of coronal spectroscopic observations, this line must be excluded from the bandpass of the coronal photometer, since there are wavelength shifts of about $\pm 0.04 \text{ \AA}$ between the east and west limb scattered

3. Kemp, J.C. (1969) J.O.S.A., 59:950.

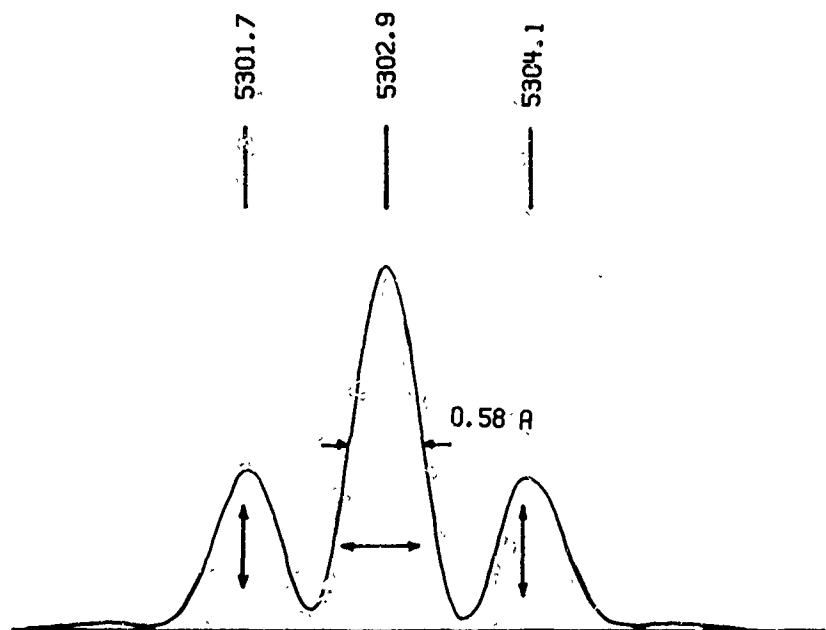


Figure 2. A Photoelectric Scan in Wavelength Showing the Photometer Transmission Profile With the Piezoelectric Modulator Operating. Arrows indicate the polarization of the transmission peaks. The time necessary to scan the profile is much longer (approximately 10 sec) than the chop rate (100 kHz)

light spectra due to solar rotation. This wavelength shift is sufficient to completely mask the coronal signal if the absorption line is located on the steep portion of the central bandpass. To avoid this problem, the filter has been tuned into the red wing of the green coronal line so that a null falls at the mean wavelength of the absorption line found in the scattered light spectrum. In fact, it has been found that when the scattered light exceeds $1000 \times 10^{-6} I_0$ (where I_0 is the mean specific intensity of the center of the solar disk) the Doppler shift of this absorption line is again detectable; $1000 \times 10^{-3} I_0$ is taken as the upper limit of sky brightness for which the photometer may be used. The integral of the central bandpass of the filter and the unshifted profiles of the green line yields

$$0.432 \int_{-\infty}^{+\infty} I_{5305}(\lambda) d\lambda = \int_{-\infty}^{+\infty} I_{\lambda 5303}(\lambda) \phi(\lambda - \lambda') d\lambda', \quad (3)$$

that is to say, only about 2/5 of the photons in the green line are detected by this system. The coronal line may also be Doppler shifted from rotational effects, but the width of the Fe XIV line makes it possible to neglect the effect.

The final tuning of the next-to-thickest element of the filter is accomplished by the rotation of a $\lambda/4$ plate just in front of the modulator. The modulator has two advantages over the usual Pockels cell found in most solar magnetographs. The angular field is quite wide; in the case of the coronal photometer, the half angle of acceptance is almost 20° . The second advantage is that the chopping rate is quite fast, 100 kHz. An early version of this photometer did use a KDP plate as a chopper, driving between $\pm \lambda/4$ with a $\lambda/4$ bias plate. The reduction in noise between this early version, which operated at 200 Hz, and the present version is a factor of 4 (see below).

3. DETECTION SYSTEM

Immediately behind the field stop is a Fabry lens that forms an image of the objective lens onto the photocathode of a PMT. The Sacramento Peak Observatory's 40-cm coronagraph is used as the feed for this photometer; the photometer is located at the east bench position in the coudé room. A schematic of the detection and control system is shown in Figure 3. The signal from the PMT is

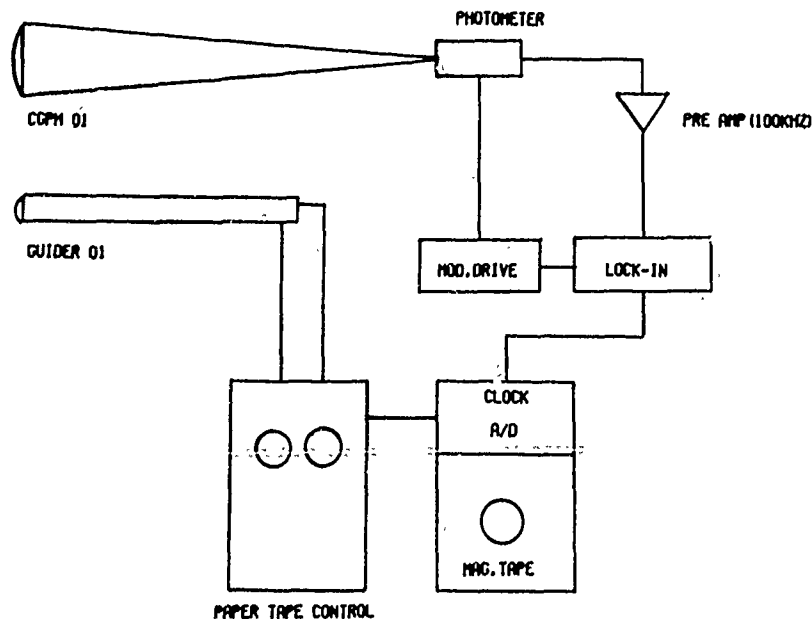


Figure 3. A Schematic Diagram of the Big Dome Spar Scan and Data Collection System as Used With the Fe XIV Photometer System

preamplified by a capacitively coupled amplifier; the signal from this is connected to the input of a modified PAR JB-4 lock-in amplifier. A reference signal is developed from the control of the modulator and this is used to phase lock onto the coronal line bandpass. Much of the gain in signal to noise between the Pockels cell version of the photometer and the present system is due to the exclusion of low frequency noise by the preamplifier. The signal from the lock-in amplifier is then digitized and recorded onto seven-track magnetic tape. The digitizer and tape recorder are controlled by punched paper tape.

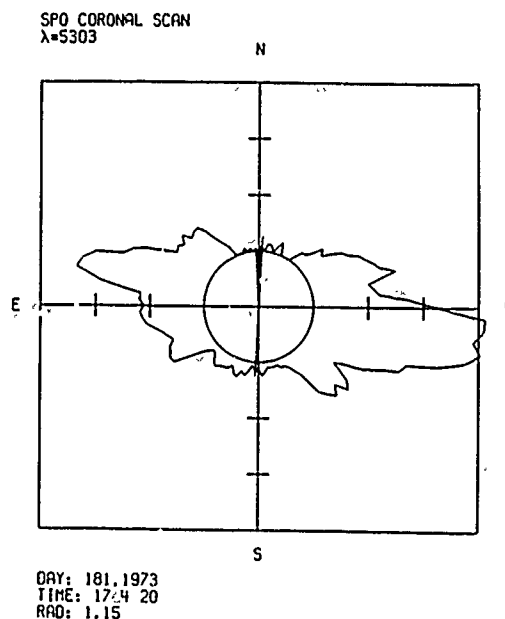
The field stop is a circular hole 3 mm in diameter, an aperture of approximately 1.1 arc minute in the field stop-image plane. The occulting disk is removed from the coronagraph and an "inverse" occulting disk, an opaque plate with a hole located at the prime focus, is used for the coronal scans. The coronagraph is offset by introducing a programmed motion into the spar guider objective. The guider servo system follows this offset and provides circular scans at distances of 1.15, 1.35, and 1.55 R/R_0 . One hundred and twenty points are sampled around the limb, every three degrees in position angle. Scans have been obtained with a radial distance of 1.75 R/R_0 from the center of the sun, but only the brightest active regions show detectable green line emission. For this reason the three-scan program outlined above is a standard observational program.

4. RESULTS

The tapes obtained during any given observing run are reduced to obtain cards (for archival storage), and one of two programs is currently used to present the data in a visual manner. The first of these programs plots a given scan in a polar presentation with a unit circle as the zero intensity level. This results in a plot that in some respects resembles a drawing of the corona, but in fact is merely a polar representation of the intensity at a given radius. The second reduction routine plots the intensity of the corona as a contour map with position angle (measured from geocentric north) along the abscissa and radius along the ordinate. A linear interpolation is used between data points in this contour routine. Examples of both kinds of plots are given in Figures 4 and 5.

Since one hundred samples of the coronal intensity in the green line of Fe XIV are taken for each scan position, it is possible to estimate the error of measurement. The noise level, in general, is proportional to the d-c level of the scattered light in the sky and instrument, and to a certain extent upon the wind loading of the spar. Observations have been obtained in situations in which the brightness of the sky just outside the limb, at the field stop, was $800 \times 10^{-6} I/I_0$ at a radial height of 1.55 R/R_0 . In this case the measure of confidence used, 1.95 σ ,

Figure 4. An Example of the Fe XIV Photometer Quick-Look-Fe-duction Program. This diagram plots $I(\lambda 5303)$ as a function of geocentric position angle at a fixed scan radius vector from the center of the solar disk. The polar rotation axis is indicated by the line through the zero intensity circle. Tic marks along the x- and y-axes indicate brightness steps of 10, 20, and $30 \times 10^{-6} I_0$.



where σ is the standard deviation of the sample at a given point, was found to be $\pm 2.5 \times 10^{-6} I/I_0$. On the other hand, the usual "noise" level for the $1.55 R/R_0$ scan in a rather ordinary sky of perhaps $200 \times 10^{-6} I/I_0$ is around $\pm 0.4 \times 10^{-6} I/I_0$. For this reason, the standard contour plot of the data uses contour levels of 1, 2, 4, 8, 16, and 32 millionths of the center of the disk intensity. It must be pointed out that the radial gradients of coronal emission lines are very high, and that a sample over 1 minute of arc area may be misleading if considered as an average brightness for the sample area in the plane of the sky.

The instrument is calibrated by pointing the coronagraph at the center of the solar disk and introducing a known attenuation into the beam. A polarizer is inserted into the photometer between the compensator plate and the $\lambda/4$ wave plate. If the axis of the polarizer is either parallel or perpendicular to the axis of the final polarizer in the system, a 100 kHz oscillation is produced, the amplitude of which is proportional to the attenuated brightness of the sun. Care must be taken to perform this calibration routine during sky circumstances that are as close to the observing period circumstances as possible, since effects of thin clouds, air mass variations, and changes in the dust or water vapor content will not be accounted for by this procedure between the period of coronal observation and the time at which the calibration routine is performed.

SACRAMENTO PEAK OBSERVATORY 5303 CORONAL INTENSITY MAP

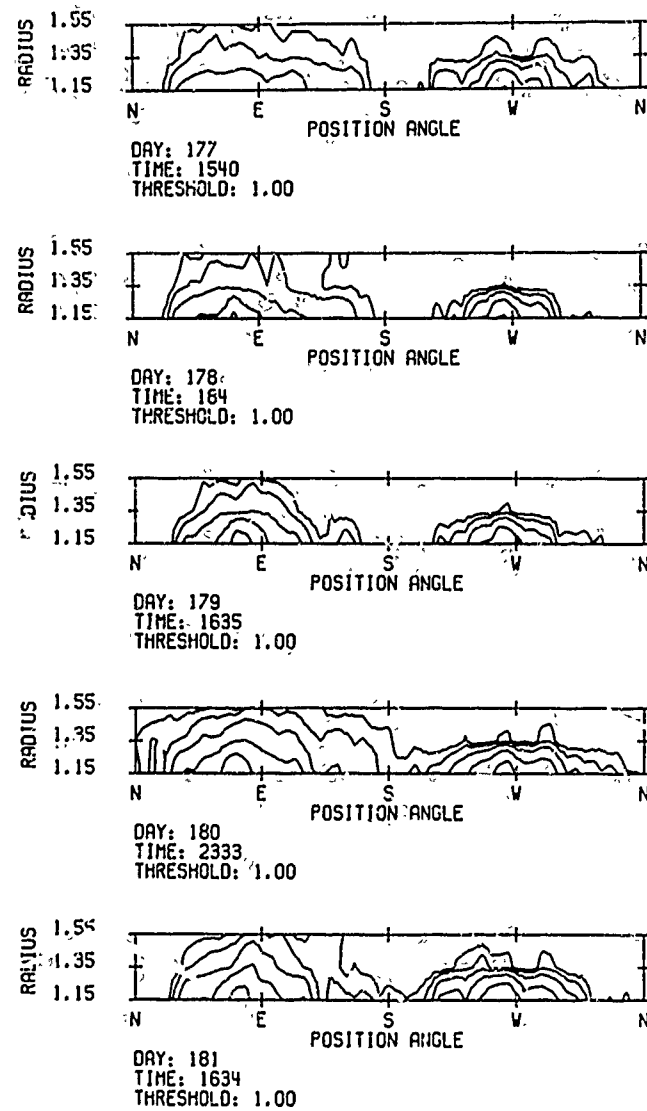


Figure 5. A Series of Five Full Coronal Scans Separated in Time by About One Day Each. The abscissa is geocentric position angle, and the ordinate is distance from the center of the disk in units of R/R_0 . Intensity is plotted in contours of 1, 2, 4, 8, and $16 \times 10^{-6} I_0$. Day 181 corresponds to the Fe XIV corona at the time of total solar eclipse, 30 June 1973

5. CONCLUSIONS

Comparison with photographs of the white light corona obtained by the author at the total solar eclipse of 1973 indicate that the 5303 Fe XIV photometer is capable of observing the major features of the active and equatorial zone corona.⁴ The narrow bandpass of the birefringent filter makes the instrument sensitive to velocity shifts of coronal material, and it is expected that observations of catastrophic activity may be compromised if the mean radial velocity of the coronal material exceeds ± 5.0 km/sec. Velocity shifts in the green line occasionally equal ± 20.0 to 25.0 km/sec in post flare loops, etc.

On the other hand, this approach to coronal observation yields data that define the average properties of the solar corona for equatorial regions over periods of observation amounting to many months. This is expected to be very useful in helping to understand the processes available for the formation of the average coronal situation at a given time. Measurements made during the three ATM missions with the green line photometer may help to fill in the portion of the corona lost behind the occulting disk of the HAO-ATM white-light coronagraph. The major advantage found to date is that the number of days during which coronal observations are available has increased over the previous photographic coverage, since the photometer is able to work in scattered light conditions in which the brightness of the sky may be 1 to 1.5 orders of magnitude greater than permitted for photographic observation of the emission line corona. This has resulted in observations during about 80 percent of the days between 1 May and 30 June 1973.

4. Fisher, R. (1973) Solar Physics, in press.